

A Lower Boundary on the Length of the Coherence Block in Vehicular Communications Channels

RAFAEL P. TORRES ¹ AND JESÚS R. PÉREZ ¹

Departamento de Ingeniería de Comunicaciones, Universidad de Cantabria, 39005 Santander, Spain

CORRESPONDING AUTHOR: JESÚS R. PÉREZ (e-mail: jesusramon.perez@unican.es)

This work was supported by the MCIN/AEI/10.13039/50110001 1033/ through the I+D+i Project under Grant PID2020-119173RB-C22.

ABSTRACT This paper presents a novel lower boundary for the coherence block (ChB) length in time-variant wireless channels. A rigorous estimation of the ChB length is important for the proper design of systems based on time division duplex-orthogonal frequency division multiplexing (TDD-OFDM). ChB length is especially relevant in the case of massive multiple input-multiple output (m-MIMO) systems, as it determines the overhead due to the massive channel estimation and, consequently, the spectral efficiency that can be achieved. The proposed boundary is based on a tractable propagation model, is related to easily obtainable channel parameters, and applicable to radio channels with temporal variation due to both the movement of the users and the movement of objects that surround them; including vehicle-to-vehicle (V2V), vehicle-to-infrastructure (V2I) and industrial Machine-to-Machine (M2M) communications.

INDEX TERMS Coherence block, massive MIMO, vehicular communications, wireless systems.

I. INTRODUCTION

The concept of the coherence block (ChB), also known in the literature as coherence interval, is fundamental for the proper design of systems based on time division duplex-orthogonal frequency division multiplexing (TDD-OFDM), and it is especially relevant in the case of massive multiple input-multiple output (m-MIMO) systems [1], [2], [3], [4], [5], [6]. The ChB length determines the overhead due to the channel estimation, and consequently, the achievable spectral efficiency that can be obtained in systems based on TDD-OFDM framework.

Considering that the channel coherence bandwidth, B_C , corresponds with the frequency interval where the channel response can be approximated as constant (flat in frequency), and the coherence time, T_C , is the time interval in which the channel is nearly time-invariant, then each coherence block contains $N_C = B_C T_C$ complex-valued samples [5], [6].

There are three important characteristics of these radio channel parameters, B_C and T_C , that should be highlighted: 1) their random nature, i.e., within the same propagation scenario both parameters vary in different local areas; and thus, a rigorous description of them must be carried out

statistically, 2) both, B_C and T_C , depend on the degree of coherence of the channel considered to define them (0.5, 0.7, or 0.9 values are the most common in the literature), and 3) the dependence of both parameters on the antenna radiation patterns [7], [8].

These three characteristics are transferred to the ChB length and must be considered when estimating ChB values in different propagation environments. A complete description of the statistical behavior of ChB length is desirable, but complex. From the point of view of its experimental analysis it is important to take into account that the measurements of the values of both T_C and B_C in a given propagation environment and in a statistically representative set of spatial points, should be undertaken simultaneously. There are sufficient experimental data for both parameters in different propagation environments, but the majority of them obtained separately, not simultaneously. The experimental acquisition of both data simultaneously has a certain complexity for outdoor environments, and not all channel sounders for measuring the broadband channel are valid for this purpose. The number of simultaneous measurements is much smaller, and they are

mostly in indoor environments, see for instance [9], [10], [11], [12], [13].

In the author's opinion, from an engineering point of view, those difficulties along with the need to manage with not very complex methodologies for the estimation of the ChB length, are the reasons why some simple approaches or rule-of-thumbs have remained as the best options for estimating ChB lengths [5], [6]. In [14], taking into account the aforementioned considerations, the authors already presented a lower boundary for the ChB length which considers its statistical behavior. This lower boundary establishes a relationship between several parameters of the channel, including the root-mean square (RMS) delay spread, τ_{RMS} , and the RMS Doppler spread, ν_{RMS} , which depends on the frequency band along with the speed of the mobile users. Furthermore, in [14] the values of the correlation levels on the ChB length, necessary to define both B_C and T_C parameters, were also considered. Likewise in [14], with a view to showing the validity and interest of the lower boundary proposed there, a statistical analysis of the behavior of ChB in an indoor environment is carried out, using a semi-empirical approach. For those purposes, in the estimation of the ChB length experimental values are used for the RMS delay, along with values obtained from a theoretical model of the RMS Doppler spread. These semi-empirical points of view could be a reasonable solution to take advantage of the large amount of experimental data which were not obtained for the purpose of estimating the length of the ChB. In [14], it is shown that the ChB length obtained for the commonly accepted rule-of-thumb [5], [6] overestimates the length of the ChB at least for correlation levels higher than 0.5.

The boundary obtained in [14] is valid for mobile channels where the transmitter and/or receiver move relative to each other, but does not consider the movement of the scatterers in the environment. From now on, we will call this the Clarke-Jakes classical mobile radio channel. The temporal variations of the channel due to the movement of the environment, the scatterers, are very significant in vehicular communications, vehicle-to-vehicle (V2V), and in the case of vehicle-to-infrastructure communications (V2I), especially in millimeter wave (mmW) bands and/or at high speeds; also, in the Internet of Things (IoT) applications in industrial environments with moving machines (M2M), and in indoor environments with a high mobility of people.

In this work, a new lower boundary for the ChB length is developed, which is applicable to mobile channels in which the transmitter, the receiver, and the environment are in movement. The new boundary maintains its simplicity; however, it is applicable to different propagation environments and systems, V2V, V2I or M2M, selecting a reduced number of model parameters. In particular, it is applicable to the propagation conditions considered in the Clarke-Jakes model, which appears as a particular case of the more general model presented here, but a tighter lower boundary for ChB than in [14] is obtained.

The proposed boundary rests on the uncertainty relationships that Bernard H. Fleury proposed and demonstrated in [15], applicable to wide-sense stationary uncorrelated scattering (WSSUS) mobile channels, which involve the pairs of parameters B_C versus τ_{RMS} , and T_C versus ν_{RMS} . These four parameters measure the extent of the channel responses in the four domains, frequency and time-delay, and, time and Doppler frequency; i.e, the four domains that describe time-varying channels from Bello's theoretical proposal [16]. However, to obtain an applicable and specific expression for the different propagation environments, it is necessary to consider a channel model that allows these parameters to be accurately estimated.

Considering the large number of existing models of time-variant channels, for the purpose at hand, it is necessary to choose a model that provides a reasonably manageable estimate of the length of the ChB, sufficiently accurate but also easily implementable. The authors have selected the model proposed in [17], because it represents a good balance between accuracy and simplicity. There exist other advanced models, for instance the proposal presented in [18], or the complete and interesting proposal shown in [19]. For the sake of brevity, and to focus on the main ideas of the paper, we refer the reader to the many references that can be found in [17], [18], [19] on the precedent and alternative time-variant channel models.

The main contributions of this work are summarized as follows:

- A new and tighter lower boundary for the ChB length is obtained. Regarding the previous one developed by the authors in [14], the new bound is more general, extending its applicability to V2V communications.
- The bound is easily applicable and depends on basic parameters of the radio channel, although it considers and emphasizes the random nature of the ChB length.
- A new probability distribution for the scatterer velocities is proposed to consider situations where signals scattered by both static and moving objects are important. The balance between both scattering sources is adjusted with a single parameter and the ChB length can be analyzed for V2V, V2I, and M2M communications in different environments.
- Finally, results are presented for two cases of V2I communications, as examples of the possibilities of the model. In all of them, it is observed that the usually accepted rules-of-thumb for estimating the ChB length overestimate its value, especially at high frequencies and velocities.

The remainder of the paper is organized as follows. Section II presents the basis for a general lower boundary for the ChB length in mobile radio channels; Section III describes the V2V channel model; Section IV includes some representative results for different V2I cases; and Section V summarizes the main conclusions that can be drawn from this work.

II. A GENERAL LOWER BOUNDARY FOR THE CHB LENGTH

It is well established that a pair of signals related by the Fourier transform (FT) verify that the width of one in a domain determines the width of the other one in the transformed domain. If the four Bello's autocorrelation functions which fully describe WSSUS mobile channels are considered, as a consequence of their FT relationships, it can be affirmed that the duration of a signal in the delay-time domain is inverse to its bandwidth in frequency; and its rhythm of time variation is inverse to the Doppler spectrum (DS) width [20], [21].

In the case of mobile radio channels, the duration of the channel response in the delay-time domain is commonly measured by the RMS delay spread, τ_{RMS} , which is calculated as the square root of the second central moment of the Power Delay Profile (PDP). It is straightforward to demonstrate that the FT of the PDP is the autocorrelation of the time-variant transfer function $H(t,f)$ with respect to the frequency variable, f . The breadth of the autocorrelation function is usually measured by the B_C at different correlation levels. Therefore, these two parameters, τ_{RMS} and B_C , will maintain an inverse relationship between them according to the compression properties of the FT [20], [21].

The relationship between B_C and τ_{RMS} has received a lot of attention since the initial contribution of Gans [22], who proposed a simple relationship:

$$B_C = \frac{1}{\alpha \tau_{RMS}} \quad (1)$$

where the parameter α depends on the shape of the PDP and the degree of correlation that defines B_C [20], [22].

Due to the duality between the Bello's functions, the RMS Doppler spread, ν_{RMS} , calculated as the square root of the second central moment of the DS, is a measure of its width; whereas the duration of the autocorrelation function in the time domain, $R(\Delta t)$, is usually measured using the coherence time, T_C , at different correlation levels. A dual relation to (1) is given in (2), in which β is a factor that depends on the DS shape and correlation level:

$$T_C = \frac{1}{\beta \nu_{RMS}}. \quad (2)$$

Furthermore, concerning pairs of functions related by the FT, the product of any length measure of one function, let us say $\langle \Delta x \rangle$, by the length of the transformed pair, $\langle \Delta y \rangle$, verifies uncertainty relations. The well-known relation $\langle \Delta x \rangle \langle \Delta y \rangle \geq 1/(4\pi)$ is verified for a pair of transformed functions when $\langle \Delta x \rangle, \langle \Delta y \rangle$ are the square root of the second central moment of such functions [21].

In [15], two uncertainty relations of great interest and applicable to WSSUS mobile channels were demonstrated, relating the durations of the basic functions of the radio channel in the four domains, as given by:

$$B_C \tau_{RMS} \geq \frac{\arccos(c_f)}{2\pi} \quad (3)$$

$$T_C \nu_{RMS} \geq \frac{\arccos(c_t)}{2\pi} \quad (4)$$

in which c_f and c_t are the correlation levels on the frequency and time domains that define B_C and T_C , respectively.

Several authors have experimentally contrasted the inequality in (3). Fleury presents in [15] the measured results of pairs (B_C, τ_{RMS}) along with the boundary defined in (3). These results were measured in an indoor environment in the 900 MHz frequency band [23]; and clearly show the fulfilment of the inequality (3). In [24], [25], results that also comply with (3) in different frequency bands and environments are presented. Concerning (4), the authors have no knowledge of their experimental confirmation, but the duality between Bello's functions is a clear indication of its validity.

By combining the two uncertainty relations (3)–(4), an inequality can be obtained which provides a general lower boundary for the duration of the ChB,

$$B_C T_C \geq \frac{\arccos(c_f) \arccos(c_t)}{4\pi^2 \tau_{RMS} \nu_{RMS}}. \quad (5)$$

An approximation to Fleury's boundaries was proposed by the authors in [14], in which τ_{RMS} and ν_{RMS} were approximated by the maximum typical values expected for the environment under analysis. Concerning the RMS delay, the inequality in (6) is considered:

$$\tau_{RMS} \leq \tau_{max}. \quad (6)$$

Moreover, considering that the DS is limited for the case of the Clarke-Jakes model by a maximum Doppler frequency value, it can be stated that:

$$\nu_{RMS} \leq \nu_{max} = \frac{v}{\lambda}. \quad (7)$$

In (7), v is the relative speed between the transmitter (Tx) and the receiver (Rx), and λ is the wavelength at the carrier frequency. From these approaches, the following lower boundary for the ChB length in mobile radio channels is obtained in [14]:

$$B_C T_C \geq \frac{\lambda \arccos(c_f) \arccos(c_t)}{4\pi^2 \tau_{max} v} \quad (8)$$

Expression (8) directly relates the minimum length of the ChB to easily measurable parameters of the mobile radio channel. However, it has the disadvantage of being too conservative, and a tighter boundary is desirable. Moreover, its applicability is restricted to the Clarke-Jakes channel, which verifies (7) and, consequently, it does not consider the movement of objects in the environment surrounding Tx and Rx.

To improve this approximation, it is proposed to maintain the limit established in (6) for τ_{RMS} , and to approximate the value of ν_{RMS} more accurately. The motivation for this approach is that the value of τ_{RMS} is highly dependent on the frequency and propagation environment, and there are no sufficiently proven analytical models to correlate this value with specific propagation environments. Taking into account the large number of available experimental data of τ_{RMS} for

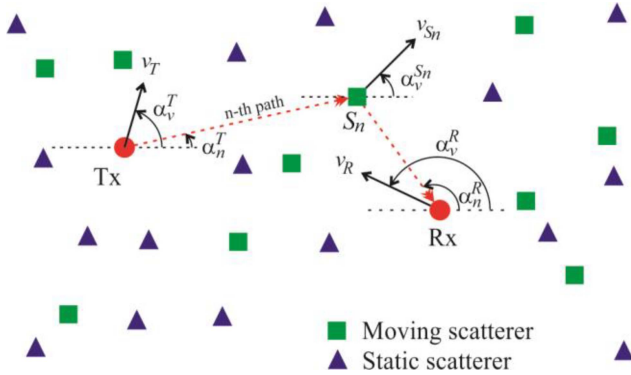


FIGURE 1. Geometric-stochastic model for the V2V channel.

different environments and frequency bands, it is more reliable to approximate them by its maximum values expected for a certain environment, τ_{max} . Therefore, the parameter τ_{max} must be obtained from measurements or site-specific models. At the same time, it is proposed to consider a more exact analytical value of the parameter v_{RMS} in (5), obtaining a more general and tighter lower boundary.

III. VEHICLE-TO-VEHICLE CHANNEL MODEL

A. GENERAL DESCRIPTION OF THE V2V MODEL

In order to obtain v_{RMS} in (5), it is proposed to use the model presented by Borhani and Pätzold in [17], which includes various propagation conditions, ranging from the already mentioned Clarke-Jakes mobile channel, fixed to fixed (F2F), V2V and M2M communications, considering the effect of the movement of the objects in the environment. As a particular case, V2I communications are included, very relevant in the case of massive MIMO systems. The selection of the model proposed in [17], is motivated by the fact that it represents a trade-off between accuracy and simplicity.

In summary, The main characteristics of the model proposed in [17] are: 1) it is an analytical model for narrowband V2V channels, which takes into account that the scatterers surrounding both Tx and Rx are moving with random velocities in random directions. It does not impose any constraint on the position of the moving scatterers; 2) the model considers general scatterer velocity distributions, which can be used to model different traffic scenarios, or machine movements in industrial environments.

Fig. 1 represents the geometric-stochastic model, showing the Tx and Rx moving with constant velocities and along defined directions in a propagation environment randomly surrounded by both static (buildings, parked cars, etc.) and moving scatterers with random velocities, v_S , and directions, α_v^S , whose statistics will be defined by its probability distribution $P(v_S)$ and $P(\alpha_v^S)$, respectively. In Fig. 1, v_T , α_v^T and v_R , α_v^R are the velocities and direction of movements of Tx and Rx, respectively; α^T and α^R stand for the angle of departure (AoD) and arrival (AoA), respectively; v_S is the speed of the scatterers and α_v^S represents their direction of movement.

B. AUTOCORRELATION FUNCTION OF THE V2V MODEL

In [17], the autocorrelation function (ACF) of the general model presented in the previous section was obtained. For that purpose, the authors considered the four Doppler spreads experienced by the signal: one due to the movement of the transmitter; the second and third ones caused by the movement of the scatterers considered as virtual receiver and transmitter; and finally, the Doppler spread due to the moving receiver. Moreover, in [17], a less general but more tractable approach is also obtained. The additional hypotheses are that: the AoD and AoA are independent and uniformly distributed between 0 and 2π . Furthermore, the direction of movement of the scatterers is considered as uniformly distributed. Under these assumptions, and as summarized in the appendix, the ACF of the V2V channel can be found in [17, Eq. (7), or Eq. (36)], and is given by:

$$R(\Delta t) = \frac{1}{4\pi^2} \int_0^\infty \int_0^{2\pi} \int_0^{2\pi} J_0(a \Delta t) e^{b \Delta t} P(v_S) d\alpha^T d\alpha^R dv_S \quad (9)$$

$$a = 2k_o v_S \cos\left(\frac{\alpha^T - \alpha^R}{2}\right) \quad (10)$$

$$b = j k_o [v_R \cos(\alpha_v^R - \alpha^R) + v_T \cos(\alpha_v^T - \alpha^T)] \quad (11)$$

where Δt represents the time lag, $J_0(\cdot)$ denotes the zeroth-order Bessel function of the first kind, and $k_o = 2\pi/\lambda$ is the free-space wavenumber. With respect to [17], the ACF in (9) has been normalized, so that $R(0) = 1$.

Starting from the ACF in (9), different known expressions are obtained for common scenarios. For the case of fixed-to-vehicle (F2V) communications without movement in the environment, $v_T = v_S = 0$, the ACF of the Clarke-Jakes model is obtained:

$$R(\Delta t) = J_0(k_o v_R \Delta t). \quad (12)$$

The ACF for a F2F radio channel surrounded by scatterers in motion is obtained from (9) considering that $v_T = v_R = 0$,

$$R(\Delta t) = \int_0^\infty J_0^2(k_o v_S \Delta t) P(v_S) dv_S. \quad (13)$$

The ACF in (13) coincides with that obtained in [26]. In the case of considering as a simplification that all the scatterers move in random directions but with the same speed, v_{S0} , then $P(v_S) = \delta(v_S - v_{S0})$, and (13) is reduced to:

$$R(\Delta t) = J_0^2(k_o v_{S0} \Delta t). \quad (14)$$

In [26], it is demonstrated that, in this case, the maximum Doppler frequency is $2v_{S0}f_0/c_0$, twice as much as in the case of the classical DS and, unlike that case, it presents a pronounced peak at the origin. Spectra with these characteristics have been measured indoors and outdoors [27], [28], [29], [30].

C. RMS DOPPLER SPREAD OF THE V2V MODEL

The RMS Doppler spread (v_{RMS}) of the channel is defined as the square root of the second central moment of the channel DS,

$$v_{RMS} = \sqrt{\overline{v^2} - (\bar{v})^2}. \quad (15)$$

The calculation of the RMS value of the DS in the Doppler frequency domain is not straightforward. However, it is simpler in the time domain, so let us consider the derivative theorem of a pair of Fourier transformed signals [21]:

$$\bar{v} = -\frac{R'(0)}{2\pi i R(0)} \quad (16)$$

where $R(\Delta t)$ is the ACF given in (9), and $R'(0)$ its first derivative at the origin. Furthermore, according to the same theorem, the following expression is obtained for the mean square value of the Doppler frequency:

$$\overline{v^2} = -\frac{R''(0)}{4\pi^2 R(0)} \quad (17)$$

in which $R''(0)$ is the second derivative of $R(\Delta t)$ at the origin.

The calculation of the first and second derivatives of the ACF is presented in the Appendix. The results of these calculations coincide with those presented in [17] although, especially concerning the second derivative, the calculations are more detailed in the Appendix.

The main results show that $R'(0) = 0$, and the second derivative evaluated at the origin is:

$$R''(0) = \frac{-2\pi^2}{\lambda^2} \left[v_R^2 + v_T^2 + 2 \int_0^\infty v_S^2 P(v_S) dv_S \right]. \quad (18)$$

It is convenient to define an effective velocity of the scatterers as:

$$v_{eff}^2 = 2 \int_0^\infty v_S^2 P(v_S) dv_S. \quad (19)$$

In this way, substituting (19) in (18) and considering (15)–(17), the following expression is obtained for the RMS value of the DS:

$$v_{RMS} = \frac{1}{\sqrt{2}\lambda} \sqrt{v_R^2 + v_T^2 + v_{eff}^2} \quad (20)$$

The expression for v_{RMS} in (20) depends on Tx and Rx velocities, as well as on the effective velocity of the scatterers, and the latter in turn on the probability distribution of the scatterer velocities $P(v_S)$. In this way, a sufficiently general expression is obtained that allows us to contemplate different traffic situations, or the movement of machines, people, etc. In [17], the expressions of the effective velocity can be found for different commonly used traffic models, such as exponential, uniform, Gaussian distributions, etc.

By substituting in (5) the value of v_{RMS} given in (20), values of the lower boundary for the ChB length are obtained, making it possible to analyze this parameter in very different

propagation environments,

$$B_C T_C \geq \frac{\sqrt{2}\lambda \arccos(c_f) \arccos(c_t)}{4\pi^2 \tau_{max} \sqrt{v_R^2 + v_T^2 + v_{eff}^2}} \quad (21)$$

IV. RESULTS: V2I CASES OF STUDY

This section includes several cases of study of interest in the context of V2I communications. These situations are useful as examples of the type of analysis that can be carried out on the duration of the ChB in different frequency bands and propagation conditions. Two propagation environments and two frequencies have been considered in this work. Concerning the environments, we will refer to urban (or pedestrian) and motorway (or in car) scenarios. Moreover, two bands intended for the deployment of 5G systems have been considered: 3.6 GHz where the first deployments have been carried out; and 26 GHz of great interest for the 5G deployment in mmW bands.

To particularize for the case of V2I communications, in the general expression given in (21), first v_T is set to zero when considering the downlink; and, taking into account the radio channel reciprocity, v_R will also be set equal to zero for the up-link. Furthermore, a model for the probability distributions of the scatterer velocities must be proposed. An original distribution is proposed that allows considering both moving scatterers, basically vehicular traffic, and fixed scatterers, such as buildings, parked cars and other street furniture:

$$P(v_S) = p \delta(v_S) + (1-p) P_0(v_S), \quad 0 \leq p \leq 1 \quad (22)$$

where $\delta(\cdot)$ denotes the Dirac's delta function and $P_0(v_S)$ represents the probability distribution of the scatterers effectively moving. It can be selected from the commonly used traffic velocity distributions: exponential, uniform, Gaussian, etc. Through the parameter p , different propagation environments can be modulated, so that the relative magnitude of scattering from fixed objects, such as buildings, parked cars, other street furniture, and the amount of scattering from moving objects, such as traffic, can be scaled to fit realistic and changing situations. For instance, focusing on the limit values of p , a value $p = 1$ corresponds with the particular case in which all the scatterers are fixed, whereas the value $p = 0$ represents just the opposite situation in which all the scatterers are moving. In our case, in order to simplify the analysis of the boundary proposed for the ChB length, we have chosen the simplest situation in which all the moving scatterers move at the same speed, v_{S0} , so (22) can be rewritten as:

$$P(v_S) = p \delta(v_S) + (1-p) \delta(v_S - v_{S0}). \quad (23)$$

In this case, the effective velocity of the scatterers is

$$v_{eff}^2 = 2(1-p)v_{S0}^2. \quad (24)$$

For the propagation conditions considered, (21) is simplified as:

$$B_C T_C \geq \frac{\sqrt{2}\lambda \arccos(c_f) \arccos(c_t)}{4\pi^2 \tau_{max} \sqrt{v_R^2 + 2(1-p)v_{S0}^2}}. \quad (25)$$

TABLE 1. Parameters of the Outdoor Situations Considered

Band	3.6 GHz			26 GHz		
	v_R (m/s)	v_S (m/s)	τ_{max} (ns)	v_R (m/s)	v_S (m/s)	τ_{max} (ns)
Urban	1.11	13.89	250	1.11	13.89	100
Motorway	27.78	27.78	250	27.78	27.78	100

In order to compare the new boundary proposed in this work with the one previously obtained by the authors in [14], it is necessary to simplify the scenario further and consider that all the scatterers are fixed, i.e., $v_{S0} = 0$, or alternatively to fix the parameter p , such that $p = 1$. For such a case, which is the only one where both boundaries are directly comparable, (25) reduces to:

$$B_C T_C \geq \frac{\sqrt{2} \lambda \arccos(c_f) \arccos(c_t)}{4\pi^2 \tau_{max} v_R}. \quad (26)$$

Comparing (26) and (8), it can be seen that the new boundary is less conservative and tighter than the old one by a factor of $\sqrt{2}$.

Table 1 shows the fundamental parameters that define the two propagation scenarios considered. These parameters include the velocities of the mobile user, i.e., the receiver, and the surrounding moving objects, i.e., the scatterers, v_R and v_S respectively; along with the maximum propagation delays expected in such environments τ_{max} . In order to select representative values for τ_{max} , experimental values of 250 and 100 ns have been considered for the 3.6 GHz [31] and 26 GHz [32] frequency bands, respectively. In the literature, more experimental works and site-specific values can be found for different environments. For the urban scenario, two different speeds are considered for pedestrian users, $v_R = 4$ km/h, and for cars, $v_S = 50$ km/h. For the motorway scenario, the same velocity is considered for users and for the surrounding traffic a speed of 100 km/h has been chosen.

In order to show the influence of the speed of mobile users, v_R , the frequency band and the degree of correlation pre-set to define B_C and T_C , the resulting ChB size for the two scenarios is presented in Fig. 2.

For simplicity, a F2V environment with static scatterers ($v_{eff} = 0$) has been considered, i.e., only the users move with the speeds proposed in Table 1. These values are obtained from (26). It is observed that the ChB size decreases with the degree of correlation required in the definition of both B_C and T_C . For example, for the urban (pedestrian) case at 26 GHz, the ChB size defined at a correlation level of 0.5 (50%) takes a value of $N_C = 4083$ samples, compared to $N_C = 2356$ for the case of a correlation level of 0.7 (70%). For the same urban case, and considering a correlation level of 0.7, the influence of the frequency is also clear, leading to a decrease in the ChB size from $N_C = 6800$, at 3.6 GHz, to $N_C = 2356$ at 26 GHz. Finally, for the correlation levels and frequencies considered, a reduction in the ChB size is observed as the speed of the

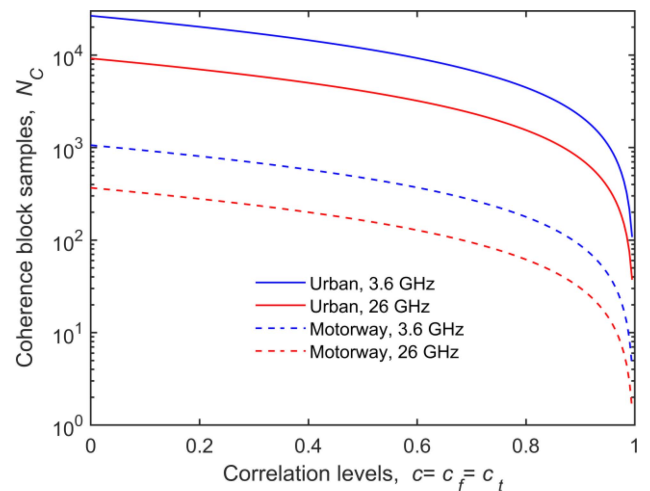


FIGURE 2. ChB length in a stationary environment for the two propagation scenarios and frequency bands considered.

TABLE 2. N_C Values: Urban Propagation Environment

		p	$c=0.5$	$c=0.7$	$c=0.9$
3.6 GHz		0	665	384	123
		0.5	940	542	174
		1.0	11797	6806	2188
26 GHz		0	230	133	43
		0.5	325	188	60
		1.0	4083	2356	757

mobile grows. In this case, for $p = 1$, the reduction is inversely proportional to the Rx velocities.

The parameter p makes it possible to weigh up the power received from each scattering source, stationary or moving. In this sense, Fig. 3 shows the ChB length obtained in the urban environment for 3.6 GHz and 26 GHz, with the parameter p ranging from 0 to 1.

The curves between these two extreme values correspond to $p = 0.2, 0.4, 0.5, 0.6$ and 0.8 . Table 2 shows the values of N_C , the ChB length, extracted from Fig. 3 for a group of representative values of p , correlation levels, c , and for both frequencies. An important reduction of N_C is observed as the Doppler power spectral density is due to a greater extent to the moving scatterers, taking the minimum value for $p = 0$.

Fig. 4 shows the results for the ChB length in the motorway environment for both frequency bands, and again considering different values for p , ranging from $p = 0$ to $p = 1$. Unlike the urban scenario presented in Fig. 3, it is observed that there is less difference between the extreme values of the parameter p , because the velocities of the user, Rx, and the traffic are the same. Moreover, a significant reduction in N_C is observed with respect to the urban case for both frequencies due to the high speeds, which obviously give rise to a clear reduction in T_C . A summary of the more representative values of N_C obtained for this scenario have been extracted from Fig. 4 and

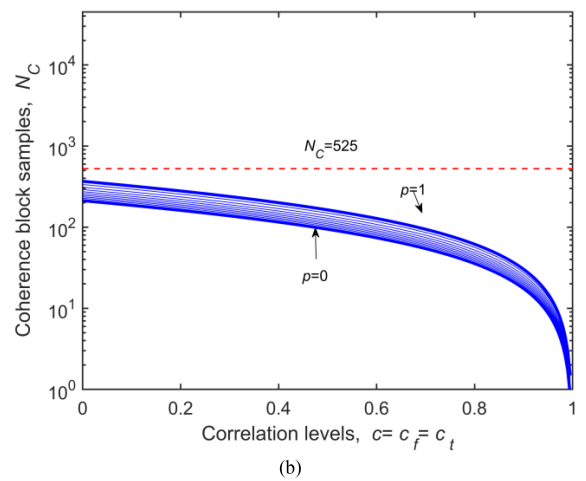
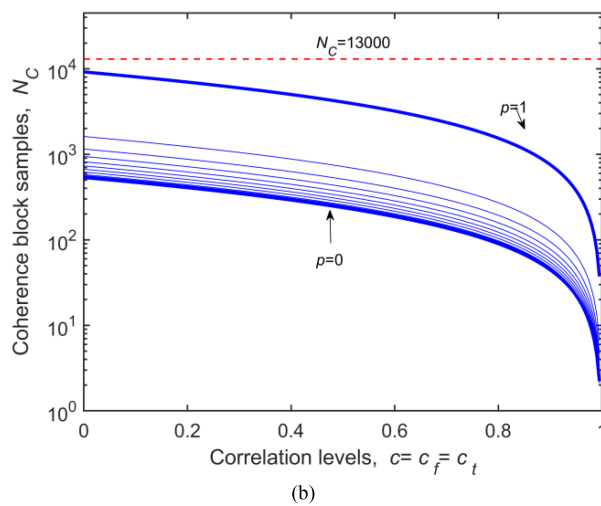
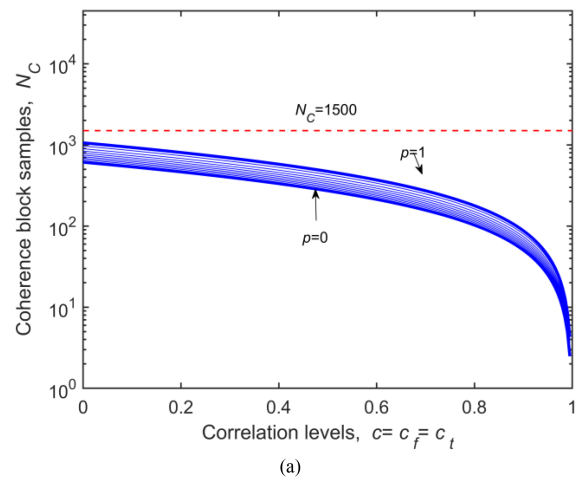
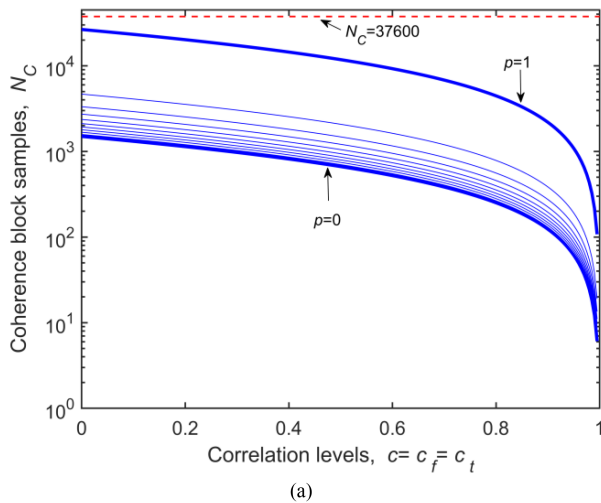


FIGURE 3. ChB length in the urban environment with $p \in [0,1]$. (a) Results for 3.6 GHz. (b) Results for 26 GHz.

TABLE 3. N_C Values: Motorway Propagation Environment

		$c=0.5$	$c=0.7$	$c=0.9$
3.6 GHz	$p=0$	272	157	50
	$p=0.5$	333	192	62
	$p=1.0$	471	272	87
26 GHz	$p=0$	94	54	17
	$p=0.5$	115	66	21
	$p=1.0$	163	94	30

are presented in Table 3 for different representative correlation levels and values of the parameter p .

Figs. 3 and 4 also show the N_C values (represented by a dashed red line) obtained using the commonly accepted rule-of-thumb [5], [6], in which N_C can be approximated by:

$$B_C = \frac{1}{2\tau_{max}} \quad (27)$$

FIGURE 4. ChB length in the motorway environment with $p \in [0,1]$. (a) Results for 3.6 GHz. (b) Results for 26 GHz.

$$T_C = \frac{\lambda}{4v} \quad (28)$$

$$N_C = B_C T_C = \frac{\lambda}{8\tau_{max} v}. \quad (29)$$

It can be observed that, obviously, N_C does not depend on the level of correlation required in the rigorous definition of T_C and B_C , and besides and more importantly, in all the cases analyzed there is an overestimation of N_C , for any correlation value. It can be seen that for a favorable case, such as an urban environment, with low speeds of mobiles and traffic, and $p = 0.5$, the overestimation in the ChB length is of the order of three times.

V. CONCLUSION

This paper presents a novel lower boundary for the coherence block length in vehicular communications channels. In comparison with the previous boundary developed by the authors, this new one has two main advantages: firstly, it is tighter, still maintaining its simplicity, which is a clear practical advantage for the design and evaluation of the physical (PHY) layer

in wireless systems; secondly, the new boundary considers the two sources of channel time variability together, one due to the relative movement between transmitter and receiver, and the second, to the movement of scatterers. The relative scattered power from both sources is easily parameterized and controlled, allowing the analysis of very general propagation conditions. In this way, the proposed boundary can be used to analyze V2V, V2I, and M2M communications in different propagation environments. The results show the impact of these two sources of time variations on the ChB length. There is a significant reduction in the ChB length for the cases in which both, mobiles and scatterers, have relatively high velocities.

The boundary explicitly relates basic parameters of the channel, such as the maximum expected RMS delay spread, carrier frequency and the velocities of mobiles and traffic. Moreover, the dependence of the length of the ChB on the selected correlation levels in order to define both B_C and T_C , is quantified. It must be pointed out that the impact of the time and frequency correlation levels on the outdated of channel estimation methods is an aspect of great interest.

The high dispersion of values of the channel parameters B_C , T_C , τ_{rms} and v_{rms} along a propagation environment underlines the need to consider the duration of the ChB as a random variable, and to analyze it from a statistical point of view, obtaining probability distributions that should allow us to obtain outage values beyond a boundary that makes it possible to ensure 100% compliance. However, since the overhead in channel estimation in future mobile communication systems, especially in systems based on massive MIMO technology, depends on the length of the ChB, the proposed lower bound is a valuable engineering tool when it comes to dimensioning and designing the physical layer.

APPENDIX

Considering the stochastic V2V channel model proposed in [17], whose formulation has been summarized in Section III, the ACF of the channel can be written according to:

$$R(\Delta t) = \frac{1}{4\pi^2} \int_0^\infty \int_0^{2\pi} \int_0^{2\pi} J_0(a \Delta t) e^{b\Delta t} P(v_S) d\alpha^T d\alpha^R dv_S \quad (A.1)$$

where:

$$a = 2k_o v_S \cos\left(\frac{\alpha^T - \alpha^R}{2}\right) \quad (A.2)$$

$$b = j k_o [v_R \cos(\alpha_v^R - \alpha^R) + v_T \cos(\alpha_v^T - \alpha^T)] \quad (A.3)$$

Taking into account that [33]:

$$\frac{d J_0(a \Delta t)}{d \Delta t} = a J_{-1}(a \Delta t) = -a J_1(a \Delta t), \quad (A.4)$$

it can be easily obtained:

$$R'(\Delta t) = \frac{1}{4\pi^2} \int_0^\infty \int_0^{2\pi} \int_0^{2\pi} (b J_0(a \Delta t) e^{b\Delta t} - a J_1(a \Delta t))$$

$$P(v_S) d\alpha^T d\alpha^R dv_S. \quad (A.5)$$

From (A.5), it is obtained that $R'(0) = 0$; considering that $J_0(0) = 1$ and $J_1(0) = 0$. Moreover, from (A.5) we proceed to the calculation of the second derivative of the ACF:

$$R''(\Delta t) = \frac{1}{4\pi^2} \int_0^\infty \int_0^{2\pi} \int_0^{2\pi} \left[e^{b\Delta t} (b^2 J_0(a \Delta t) - 2ab J_1(a \Delta t) - \frac{a^2}{2} (J_0(a \Delta t) - J_2(a \Delta t))) \right] \times P(v_S) d\alpha^T d\alpha^R dv_S. \quad (A.6)$$

To obtain (A.6) it has been considered that [33]:

$$J_1'(a \Delta t) = \frac{a}{2} (J_0(a \Delta t) - J_2(a \Delta t)). \quad (A.7)$$

From (A.6) we obtain the value of $R''(\Delta t)$ at the origin, i.e., $\Delta t = 0$, given by:

$$R''(0) = \frac{1}{4\pi^2} \int_0^\infty \int_0^{2\pi} \int_0^{2\pi} \left(b^2 - \frac{a^2}{2} \right) P(v_S) d\alpha^T d\alpha^R dv_S \quad (A.8)$$

Substituting the values of a and b in (A.8), and considering [17, Eq. (29)] along with the uniform distribution of α^T and α^R , we finally obtain:

$$R''(0) = \frac{-2\pi^2}{\lambda^2} \left[v_R^2 + v_T^2 + 2 \int_0^\infty v_S^2 P(v_S) dv_S \right]. \quad (A.9)$$

In this Appendix:

α^T	stands for the angle of departure, AoD.
α^R	stands for the angle of arrival, AoA.
v_S	is the speed of the scatterers.
v_R	is the speed of the mobile user.
α_v^S	represents the direction of movement of scatterers.
$k_o = 2\pi/\lambda$,	is the free-space wavenumber.
$P(v_S)$	stands for the probability distribution of the v_S for the scatterers.
$R(\Delta t)$	is the ACF.
$R'(\Delta t)$	is the first derivative of the ACF.
$R''(\Delta t)$	is the second derivative of the ACF.

REFERENCES

- [1] T. L. Marzetta, "How much training is required for multiuser MIMO?," in *Proc. IEEE 40th Asilomar Conf. Signals, Syst. Comput.*, Pacific Grove, CA, USA, Oct. 2006, pp. 359–363, doi: [10.1109/ACSSC.2006.354768](https://doi.org/10.1109/ACSSC.2006.354768).
- [2] T. L. Marzetta, "Noncooperative cellular wireless with unlimited numbers of base station antennas," *IEEE Trans. Wirel. Comm.*, vol. 9, no. 11, pp. 3590–3600, Nov. 2010, doi: [10.1109/TWC.2010.092810.091092](https://doi.org/10.1109/TWC.2010.092810.091092).
- [3] E. Björnson, E. G. Larsson, and T. L. Marzetta, "Massive MIMO: Ten myths and one critical question," *IEEE Comm. Mag.*, vol. 54, no. 2, pp. 114–123, Feb. 2016, doi: [10.1109/MCOM.2016.7402270](https://doi.org/10.1109/MCOM.2016.7402270).
- [4] E. Björnson, E. G. Larsson, and M. Debbah, "Massive MIMO for maximal spectral efficiency: How many users and pilots should be allocated?," *IEEE Trans. Wirel. Comm.*, vol. 15, no. 2, pp. 1293–1308, Feb. 2016, doi: [10.1109/TWC.2015.2488634](https://doi.org/10.1109/TWC.2015.2488634).
- [5] T. L. Marzetta, E. G. Larsson, H. Yang, and H. Q. Ngo, *Fundamentals of Massive MIMO*. Cambridge, U.K., MA, USA, Cambridge Univ. Press, 2016.

- [6] E. Björnson, J. Hoydis, and L. Sanguinetti, "Massive MIMO networks," in *Massive MIMO Networks: Spectral, Energy, and Hardware Efficiency*, PW Delft, The Netherlands: Now Publishers, 2017, ch. 2, pp. 219–220.
- [7] J. R. Pérez and R. P. Torres, "On the impact of the radiation pattern of the antenna element on MU-MIMO indoor channels," *IEEE Access*, vol. 8, pp. 25459–25467, 2020, doi: [10.1109/ACCESS.2020.2970769](https://doi.org/10.1109/ACCESS.2020.2970769).
- [8] V. Va, J. Choi, and R. W. Heath, "The impact of beamwidth on temporal channel variation in vehicular channels and its implications," *IEEE Trans. Veh. Tech.*, vol. 66, no. 6, pp. 5014–5029, Jun. 2017, doi: [10.1109/TVT.2016.2622164](https://doi.org/10.1109/TVT.2016.2622164).
- [9] A. Abdelgawad, A. Borhani, and M. Pätzold, "Modelling, analysis, and simulation of the micro-Doppler effect in wideband indoor channels with confirmation through pendulum experiments," *Sensors*, vol. 20, no. 4, Feb. 2020, Art. no. 1049, doi: [10.3390/s20041049](https://doi.org/10.3390/s20041049).
- [10] A. Borhani, M. Pätzold, and K. Yang, "Time-frequency characteristics of in-home radio channels influenced by activities of the home occupant," *Sensors*, vol. 19, no. 16, Aug. 2019, Art. no. 3557, doi: [10.3390/s19163557](https://doi.org/10.3390/s19163557).
- [11] F. Burmeister, N. Schwarzenberg, T. Hößler, and G. Fettweis, "Measuring time-varying industrial radio channels for D2D communications on AGVs," in *Proc. 2021 IEEE Wireless Commun. Netw. Conf.*, Nanjing, China, 2021, pp. 1–7, doi: [10.1109/WCNC49053.2021.9417520](https://doi.org/10.1109/WCNC49053.2021.9417520).
- [12] D. Morejón, E. Iradier, P. Angueira, and J. Montalban, "Empirical delay and Doppler profiles for industrial wireless channel models," in *Proc. IEEE 19th Int. Conf. Factory Comm. Syst.*, Pavia, Italy, 2023, pp. 1–4, doi: [10.1109/WFCS57264.2023.10144250](https://doi.org/10.1109/WFCS57264.2023.10144250).
- [13] R. Candell et al., "Industrial Wireless Systems: Radio Propagation Measurements," *Tech. Note (NIST TN)*, Nat. Inst. Standards Technol., Gaithersburg, MD, Jan. 2017. Accessed: Dec. 18, 2024. [Online]. Available: <https://doi.org/10.6028/NIST.TN.1951>
- [14] R. P. Torres and J. R. Pérez, "A lower bound for the coherence block length in mobile radio channels," *Electronics*, vol. 10, no. 4, Feb. 2021, Art. no. 398, doi: [10.3390/electronics10040398](https://doi.org/10.3390/electronics10040398).
- [15] B. H. Fleury, "An uncertainty relation for WSS processes and its application to WSSUS systems," *IEEE Trans. Comm.*, vol. 44, no. 12, pp. 1632–1634, Dec. 1996, doi: [10.1109/26.545890](https://doi.org/10.1109/26.545890).
- [16] P. Bello, "Characterization of randomly time-variant linear channels," *IEEE Trans. Comm. Sys.*, vol. 11, no. 4, pp. 360–393, Dec. 1963, doi: [10.1109/TCOM.1963.1088793](https://doi.org/10.1109/TCOM.1963.1088793).
- [17] A. Borhani and M. Pätzold, "Correlation and spectral properties of vehicle-to-vehicle channels in the presence of moving scatterers," *IEEE Trans. Veh. Tech.*, vol. 62, no. 9, pp. 4228–4239, Nov. 2013, doi: [10.1109/TVT.2013.2280674](https://doi.org/10.1109/TVT.2013.2280674).
- [18] W. Dahech, M. Pätzold, C. A. Gutiérrez, and N. Youssef, "A non-stationary mobile-to-mobile channel model allowing for velocity and trajectory variations of the mobile stations," *IEEE Trans. Wirel. Comm.*, vol. 16, no. 3, pp. 1987–1999, Mar. 2017, doi: [10.1109/TWC.2017.2659723](https://doi.org/10.1109/TWC.2017.2659723).
- [19] C. A. Gutiérrez, R. A. Fabián-Rodríguez, F. R. Castillo-Soria, C. A. Azurdia-Meza, and P. Adasme, "SOC-based simulation of 3D MIMO mobile-to-mobile fading channels: A Riemann sum approach," *IEEE Open J. Veh. Tech.*, vol. 5, pp. 1–20, 2024, doi: [10.1109/OJVT.2023.3331534](https://doi.org/10.1109/OJVT.2023.3331534).
- [20] J. D. Parsons, "Wideband channel characterization," in *The Mobile Radio Propagation Channel*, 2nd ed., Chichester, U.K.: Wiley, 2000, ch. 6, pp. 164–189.
- [21] R. N. Bracewell, "The two domains," in *The Fourier Transform and Its Applications*, 2nd ed., Singapore: McGraw-Hill, 1978, ch.8, pp. 135–163.
- [22] M. J. Gans, "A power-spectral theory of propagation in the mobile-radio environment," *IEEE Trans. Veh. Tech.*, vol. 21, no. 1, pp. 27–38, Feb. 1972, doi: [10.1109/TVT.1972.23495](https://doi.org/10.1109/TVT.1972.23495).
- [23] E. Zollinger, "Measured inhouse radio wave propagation characteristics for wideband communication systems," in *Proc. IEEE 8th Eur. Conf. Electrotechnics, Conf. Proc. Area Commun.*, Stockholm, Sweden, 1988, pp. 314–317, doi: [10.1109/EURCON.1988.11165](https://doi.org/10.1109/EURCON.1988.11165).
- [24] N. Moraitis, A. Kanatas, G. Pantos, and P. Constantinou, "Delay spread measurements and characterization in a special propagation environment for PCS microcells," in *Proc. IEEE Int. Symp. Pers., Indoor Mobile Radio Comm.*, Lisboa, Portugal, 2002, pp. 1190–1194, doi: [10.1109/PIMRC.2002.1045216](https://doi.org/10.1109/PIMRC.2002.1045216).
- [25] J. R. Pérez et al., "Empirical characterization of the indoor radio channel for array antenna systems in the 3 to 4 GHz frequency band," *IEEE Access*, vol. 7, pp. 94725–94736, 2019, doi: [10.1109/ACCESS.2019.2928421](https://doi.org/10.1109/ACCESS.2019.2928421).
- [26] S. Thoen, L. Van der Perre, and M. Engels, "Modeling the channel time-variance for fixed wireless communications," *IEEE Comm. Lett.*, vol. 6, no. 8, pp. 331–333, Aug. 2002, doi: [10.1109/LCOMM.2002.802044](https://doi.org/10.1109/LCOMM.2002.802044).
- [27] R. J. C. Bultitude, R. F. Hahn, and R. J. Davies, "Propagation considerations for the design of an indoor broad-brand communications system at EHF," *IEEE Trans. Veh. Tech.*, vol. 47, pp. 235–245, Feb. 1998, doi: [10.1109/25.661050](https://doi.org/10.1109/25.661050).
- [28] S. J. Howard and K. Pahlavan, "Doppler spread measurements of the indoor radio channels," *Electron. Lett.*, vol. 26, no. 2, pp. 107–109, Jan. 1990, doi: [10.1049/el:19900074](https://doi.org/10.1049/el:19900074).
- [29] H. Hashemi, M. McGuire, and D. Tholl, "Measurements and modeling of temporal variations of the indoor radio propagation channel," *IEEE Trans. Veh. Tech.*, vol. 43, pp. 733–737, Aug. 1994, doi: [10.1109/25.312774](https://doi.org/10.1109/25.312774).
- [30] R. P. Torres, B. Cobo, D. Mavares, F. Medina, S. Loredó, and M. Engels, "Measurement and statistical analysis of the temporal variations of a fixed wireless link at 3.5 GHz," *Wirel. Pers. Commun.*, vol. 37, no. 1, pp. 41–59, Apr. 2006, doi: [10.1007/s11277-006-1320-z](https://doi.org/10.1007/s11277-006-1320-z).
- [31] Z. Wang, P. Wang, W. Li, and H. Xiong, "Wideband channel measurements and characterization of the urban environment," in *Proc. IEEE Int. Symp. Microw., Antenna, Propagat. EMC Tech. Wireless Commun.*, Hangzhou, China, Aug. 2007, pp. 826–829, doi: [10.1109/MAPE.2007.4393752](https://doi.org/10.1109/MAPE.2007.4393752).
- [32] T. S. Rappaport, G. R. MacCartney, M. K. Samimi, and S. Sun, "Wideband millimeter-wave propagation measurements and channel models for future wireless communication system design," *IEEE Trans. Comm.*, vol. 63, no. 9, pp. 3029–3056, Sep. 2015, doi: [10.1109/TCOMM.2015.2434384](https://doi.org/10.1109/TCOMM.2015.2434384).
- [33] M. Abramowitz and I. A. Stegun, "Bessel functions of integer order," in *Handbook of Mathematical Functions*, 9th ed., New York, NY, USA: Dover Publications, Inc., 1972, ch 9, pp. 358–360.



RAFAEL P. TORRES received the M.S. degree in physics from the Universidad de Granada, Spain, in 1986, and the Ph.D. degree in telecommunications engineering from the Universidad Politécnica de Madrid, Madrid, Spain, in 1990. He was an Associate Professor with the Department of Communications Engineering, Universidad de Cantabria, Santander, Spain, where he is currently a Full Professor in Signal Processing and Communications Engineering. His fundamental lines of research have been development of numerical methods for

the analysis and design of antennas, application of high frequency techniques for simulation and analysis of the radar section, as well as the design of radar systems. From the end of the nineties, his research focuses on the study, modelling and measurement of the radio channel and the analysis of its impact on mobile and wireless communications systems. Main achievements focus on the development of ray-tracing methods to simulate the radio channel in complex propagation environments, on the experimental characterization of the channel, both SISO and MIMO, and on the development of space-time coding techniques.



JESÚS R. PÉREZ received the B.Sc., M.Sc. and Ph.D. degrees in telecommunications engineering from the Universidad de Cantabria, Santander, Spain, in 1996, 1999 and 2005, respectively. He joined the Department of Communications Engineering, Universidad de Cantabria in 1999 and he was awarded a Graduate Research and a Post-Doctoral grant in 2002 and 2006, respectively. He was an Associate Professor in 2009. His research interests include radio propagation and measurement techniques for the experimental characterization of the radio channel, computational electromagnetics and optimization methods.